

# Properties of Injection Molded Nanocomposites and Blends Based on PLA, PHBV and L-CNC

Martin Borůvka<sup>1\*</sup>, Luboš Běhálek<sup>1</sup>, Jiří Habr<sup>1</sup>, Petr Lenfeld<sup>1</sup>,  
Jan Vácha<sup>1</sup>, Chakaphan Ngaowthong<sup>2,3</sup>

<sup>1</sup>Department of Engineering Technology, Technical University of Liberec,  
Studentská 2, 461 17 Liberec 1, Czech Republic.

<sup>2</sup>The Sirindhorn International Thai – German Graduate School of  
Engineering (TGGS), King Mongkut's University of Technology North  
Bangkok, 1518 Pracharat 1 Road, Bangsue, Bangkok 10800, Thailand.

<sup>3</sup>Faculty of Industrial Technology and Management, King Mongkut's  
University of Technology North Bangkok Prachinburi Campus, 29 Moo 6,  
Tumbon Noenhom, Amphur Muang, Prachinburi 25230, Thailand.

\*[martin.boruvka@tul.cz](mailto:martin.boruvka@tul.cz)

## ABSTRACT

*The practical approach to produce sustainable, biobased, biodegradable and ecofriendly blends and nanocomposites with tailored material properties is reported in this paper. The aim of study is to investigate the effect of blending and addition of heterogeneous nucleating agents based on lignin-coated cellulose nanocrystals (L-CNCs) on the properties of poly(lactic acid) (PLA) and poly(3-hydroxybutyrate-co-3-hydroxyvalerate) (PHBV) blends and nanocomposites. The crystallization behaviour, morphology, impact strength and heat deflection temperature of neat PLA, blends and nanocomposites were investigated. Masterbatches were prepared by melt mixing using an internal mixer and further then were standard tensile test bars injection molded. The results showed that both property modifiers (PHBV and L-CNC) had significant influence on PLA material properties. Crystallinity of resulted samples has been improved. Morphology examinations showed PHBV well dispersed in PLA phase in form of droplet like particles in nanometre range. An increase of impact strength and heat deflection temperature (HDT) has been observed.*

**Keywords:** *poly (lactic acid); poly (hydroxybutyrate-co-hydroxyvalerate); lignin-coated cellulose nanocrystals; biopolymer blends, nanocomposites*

## **Introduction**

Increasing interest in biobased and biodegradable polymers is primarily caused by rising concerns over environmental issues, sustainability and dependency on decreasing petroleum resources [1]. The interest on these biopolymers is also considerable in the prospect of limiting plastics waste disposal through non-toxic degradation [2].

The most commonly used biopolymer, poly(lactic acid) (PLA) can be synthesized by either ring-opening polymerization of lactide or condensation polymerization of lactic acid monomers that are produced from renewable resources such as corn and sugarcane via fermentation process [3]. PLA is biobased, biodegradable and biocompatible aliphatic thermoplastic polyester with excellent melt-processability, transparency, high strength (50-70 MPa) and modulus (3 GPa). In addition, PLA is industrially scalable and commercially available at affordable cost. It has been studied and used in a wide variety of applications such as packaging, biomedical and automotive [4]. However, still faces important industrial problems such as a slow crystallization rate, hydrolytic degradation, low thermal stability and inherent brittleness to compete with synthetic commodity polymers [5]. With a view of sustainable development of science and technology, these problems need to be improved in order to widen PLA application possibilities.

The effective, practical and economical concept how to improve polymer properties is blending with other polymers. Incorporation of biobased and biodegradable polymers is desired in development of sustainable polymer blends [6]. Blending can substantially modify PLA mechanical and thermal properties, biodegradation rate and permeability [7]. Polyhydroxyalkanoates (PHAs) belongs to a group of linear polyesters that are produced in nature by bacterial fermentation of sugars and lipids. They are synthesized as intracellular carbon storage compounds and energy reserves in a various bacteria. PHAs are widely used in various biomedical applications due to their excellent biocompatibility and biodegradability [8]-[9]. The most important PHAs are poly(3-hydroxybutyrate) (PHB) and poly(3-hydroxybutyrate-co-3-hydroxyvalerate) (PHBV). PHB is a highly crystalline and brittle polymer with high melting point and stiffness. To enhance higher flexibility and melt processing capabilities is PHB copolymerized with 3-hydroxyvalerate (HV). Resulting PHBV is a copolymer of PHB with randomly arranged 3-hydroxybutyrate (HB) groups and 3-hydroxyvalerate (HV) groups [6]-[9]-[10]. Copolymer shows increase of elongation at break, lowering of Young's modulus, crystallinity and melting temperature with increasing HV group

content [11]. Several authors focused their efforts to improve properties of PLA via blending with various PHAs [6]-[9]-[12]-[13]-[14]-[15]. Conventional processing (injection molding and thermoforming) results industrially in PLA products with very low crystallinity state.

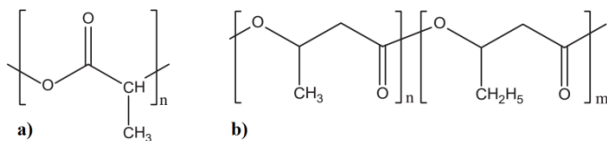


Figure 1: Chemical structure of PLA (a) and PHBV (b) [16]

An efficient approach how to improve PLA properties, especially crystallization rate through increasing nucleation density during industrial processing is incorporation of heterogeneous nucleating agents [17]-[18]. However, there are several types of heterogeneous nucleating agents used in PLA processing, those based on biobased resources with triggered biodegradability and biocompatibility are highly desired. Several authors used biobased nucleants to enhance crystallization rate of PLA [3]-[19]-[20].

Cellulose nanocrystals (CNCs) are one of the most emerging and promising heterogeneous nucleants for PLA due to their interesting properties and biobased origin. Cellulose ( $C_6H_{11}O_5$ )<sub>n</sub> is a linear chain polysaccharide and most abundant organic compound affecting the Earth's surface. In nature exist in form of cellulose microfibrils, formed by side-by-side arrangement of strings of cellulose crystallites, linked along the chain axis by amorphous domains. CNCs are produced using a top-down mechanically or chemically induced deconstructing strategy of hierarchical cellulose structure by hydrolysis of amorphous domains. Typical dimensions of CNCs ranging from 3-5 nm in width and 50-500 nm in length. CNC have unique properties such as high axial stiffness (~ 150 GPa), high tensile strength (~ 7.5 GPa), low coefficient of thermal expansion (~ 1 ppm/K), thermal stability up to ~ 300 °C, high aspect ratio (~ 10-100), low density (~ 1.6 g/cm<sup>3</sup>) and reactive surface composed of hydroxyl groups (-OH) [21]-[22]-[23]. In despite of those interesting properties, poor dispersion and distribution of CNCs in PLA limit the potential of mechanical reinforcement and nucleation density capabilities. Intra- and inter-molecular hydrogen bonds between CNCs tend to form bundles in presence of non-polar polymers like PLA.

Different strategies has been reported to solve this problem, among them the most promising are silanization, grafting of PLA on CNCs surface based on the “grafting from” approach, i.e., a surface-initiated ring opening polymerization (SI-ROP) and lignin coating [5]-[24]-[25]-[26]-[27]. In this paper, novel, commercially available and biobased hydrophobic lignin coated cellulose nanocrystals (L-CNCs) has been used. The single commercial-scale

process and cost-effective production of CNC with possibilities of lignin coated hydrophobic versions (L-CNC) was developed by American Process Inc. (API) (USA). Thin layer of lignin is deposited through electrostatic and Van der Waals interaction on CNCs surface and further than are L-CNCs spray dried [22].

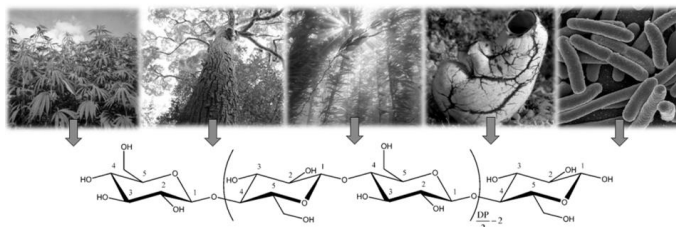


Figure 2: Examples of cellulose-synthesizing organisms and cellulose chemical structure [28]

## Experimental

### Materials

Commercial grade PLA (Ingeo™ 3251D) in pellet form was purchased from Nature Works LLC (USA). PHBV (ENMAT™ Y1000P) in powder form was purchased from Tianan Biologic Material Company LTD. (China). Spray dried lignin coated cellulose nanocrystals (L-CNC) (BioPlus-L™ Crystals) having an average particle size of 4-5 nm in width and 50-500 nm in length was purchased from American Process Inc. (USA).

### Processing

The aim of the study was to use PLA as primary matrix material and PHBV and L-CNC as property modifiers. Prior to processing, PLA pellets were dried overnight in laboratory oven (55°C, 12 h.). PHBV and L-CNC powders were dried in an oven at 70°C overnight. Pure PLA, PLA/PHBV blends, PLA/L-CNC nanocomposites and PLA/PHBV/L-CNC nanocomposite blends were prepared by melt mixing using a CT Internal Mixer (MX 75) (Thailand) equipped with roller type rotors. At first PLA pellets were added to mixing chamber at temperature 170°C with a rotor speed 50 rpm. Further than in case of blends were added powdered PHBV, L-CNC in case of nanocomposites and both in case of nanocomposite blends to reach desired concentrations. Samples were let mixing for 7-10 min until steady state torque was reached. Pure PLA masterbatch was prepared in same way to undergo same preparation conditions. For each sample type were prepared 300 g masterbatches. Masterbatches were then crushed at shear mill (RETSCH SM 300) (Germany) to pellet like particle size and mixed in desired concentration with pure PLA

pellets. Prior to injection molding were materials dried in Maguire Low Pressure Dryer (LPD 100) (USA) under the following conditions: temperature 80 °C, time 240 min, vacuum 0.8 bar. Standard tensile test bars were injection molded according to ISO 527 on injection molding machine (ARBURG 270S 400-100) (Germany) with increasing temperature profile (165 °C up to 190 °C) of the melting chamber.

Resulted samples are depicted under code names with final concentrations in Table 1. In case of nanocomposite blends was 1 wt. % of L-CNCs in a final blend mixture calculated always over 100 wt. % of a blend.

Table 1: PLA, nanocomposites and nanocomposite blends concentrations

Sample Code	Composition (wt.%)		
	PLA	PHBV	L-CNC
PLA	100	-	-
PLA/L-CNC (99/1)	99	-	1
PLA/PHBV (90/10)	90	10	-
PLA/PHBV/L-CNC (90/10/1)	90	10	1
PLA/PHBV (80/20)	80	20	-
PLA/PHBV/L-CNC (80/20/1)	80	20	1

## Characterization

Study of crystallization was conducted by differential scanning calorimetry (DSC) Mettler Toledo DSC 1/700 calorimeter (Switzerland) according to ISO 11357. The samples amount 8 - 11 mg were sealed in an aluminium pan and heated to 200 °C and kept isothermal for 5 min to remove previous thermal history, then cooled again. The second heating-cooling cycle analysis run at 10 °C min<sup>-1</sup> heating/cooling ramp in a nitrogen atmosphere (flow rate 50 ml·min<sup>-1</sup>) to determine thermal transitions: glass transition ( $T_g$ ), cold crystallization ( $T_{cc1}$  and  $T_{cc2}$ ) and melting ( $T_f$ ) temperatures and enthalpies ( $\Delta H_{cc1}$ ,  $\Delta H_{cc2}$ ,  $\Delta H_f$ ). Since PLA 3251D is designed for high melt flow applications and has very slow nucleation and crystallization rates, the samples have very low degree of crystallinity. The crystalline fraction  $\chi_c$  (%) of PLA, blends and nanocomposite samples was calculated by following equation [29]:

$$\chi_c(\%) = \frac{\Delta H_f - \Delta H_{cc}}{\Delta H_f^0 \cdot W_m} \times 100 \quad (1)$$

where  $\Delta H_f$  is enthalpy of fusion and  $\Delta H_{cc}$  is enthalpy of cold crystallization, both determined by DSC.  $\Delta H_f^0$  is melting enthalpy of 100% crystallized polymer (PLA:  $\Delta H_f^0 = 93 \text{ J} \cdot \text{g}^{-1}$  [30] and

PHBV:  $\Delta H_f^0 = 109 \text{ J} \cdot \text{g}^{-1}$  [31]) and  $W_m$  is the weight fraction of PLA and PHBV in blend.

The total theoretical enthalpy of fusion  $\Delta H_f$  of blends can be calculated according to additive mixing rule expressed by equation (2).

$$\Delta H_f = \Delta H_{f-PLA} \cdot W_{m-PLA} + \Delta H_{f-PHBV} \cdot W_{m-PHBV} \quad (2)$$

where  $\Delta H_{f-PLA}$  and  $\Delta H_{f-PHBV}$  are the enthalpies of melting of pure PLA and PHBV measured by DSC,  $W_{m-PLA}$  and  $W_{m-PHBV}$  are weight fraction of PLA and PHBV in a blend. For most of the blends the experimental data coincide with the theoretical enthalpy calculated according to the simple mixing rule.

The scanning electron microscope (SEM) examination of prepared samples was conducted on Carl Zeiss ULTRA Plus (Germany). Examined surfaces were taken from middle cross-section of cryo-fractured tensile bars.

Impact properties of injection molded tensile bars were prepared and measured according to ISO 179-1/1eU (unnotched) on CEAST Resil 5.5 (Italy) at room temperature 23°C.

The Heat Deflection Temperature (HDT) measurements were conducted according to ISO 75 (method A) on HDT-KSP analyzer (Czech Republic) at heating rate of 120°C h<sup>-1</sup>. Samples were heated from room temperature to desired temperature in a three point bending cantilever.

## **Results and discussion**

### **DSC**

Differential scanning calorimetry was used to investigate the effect of blending and addition of heterogeneous nucleating agents based on L-CNCs on the glass transition, non-isothermal crystallization and melting phenomena of blends, nanocomposites and nanocomposite blends. Resulted DSC scans (Figure 3) were taken from second heating step to remove previous thermal history of sample processing. Cooling scans are depicted in Figure 4 and thermal parameters are summarized in Table 2. During heating of samples was observed the glass transition temperature ( $T_g$ ), the primary peak cold crystallization temperature ( $T_{cc1}$ ), further secondary peak cold crystallization temperature ( $T_{cc2}$ ) and melting temperature ( $T_m$ ). Cold crystallization ( $\Delta H_{cc}$ ) (recrystallization) is represented by exothermic peak that is caused by absorbed enthalpy during crystal growth. Such cold crystallization of material is related to rapid cooling of the melt in the mould cavity during industrial injection molding process. It negatively influenced not only the structure change and material properties but also shape and dimensional instabilities of injected parts. Results of second heating scans are depicted in Figure 3, cooling scans are depicted in Figure 4 and thermal parameters are summarized in Table 2.

Slight decrease of  $T_g$  of PLA from 60,7°C for pure PLA to 57±0,5 for PLA/PHBV blends and PLA/PHBV/L-CNC nanocomposite blends has been observed during second heating scan (Figure 3). This decrease of  $T_g$  can be understood as an increase of compatibility or partial miscibility of PLA/PHBV blends due to shift of PLA  $T_g$  towards PHBV  $T_g$  (around 5°C). Same decrease has been observed by Gerard and Budtova [12]. As can be seen in Figure 3 addition of L-CNC (1 wt. %) increases the degree of crystallinity ( $\chi_c$ ) but also lowers the cold crystallization enthalpy ( $\Delta H_{cc}$ ) which slips to the lower temperatures or more precisely it lowers its temperature interval. An increase of  $\chi_c$  from 4,6 % for pure PLA to 10.1 % for PLA/L-CNC has been observed. Degree of crystallinity calculation of PLA phase and PHBV phase in blends and PLA/PHBV/L-CNC nanocomposite blends is due to overlapping of melting enthalpies ( $\Delta H_f$ ) challenging and both equation (1) and equation (2) has been applied. However this calculations are not precise and results need to be verified by X-ray Diffraction (XRD) in further studies. Even higher shift to lower temperatures has been observed in cold crystallization peak for both PLA/PHBV blends and PLA/PHBV/L-CNC nanocomposite blends can be seen in Figure 3 and Table 2. In the cooling scans (Figure 4), the exothermic peaks with nearly no intensity were observed for all samples based on PLA, indicating a rather low crystallization capability.

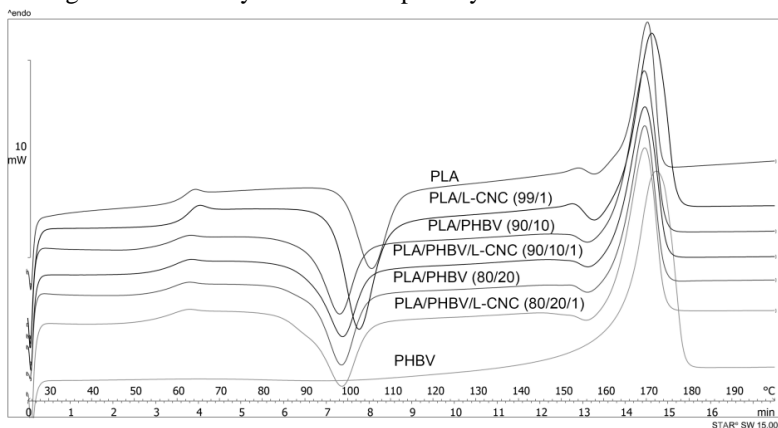


Figure 3: DSC second heating scans

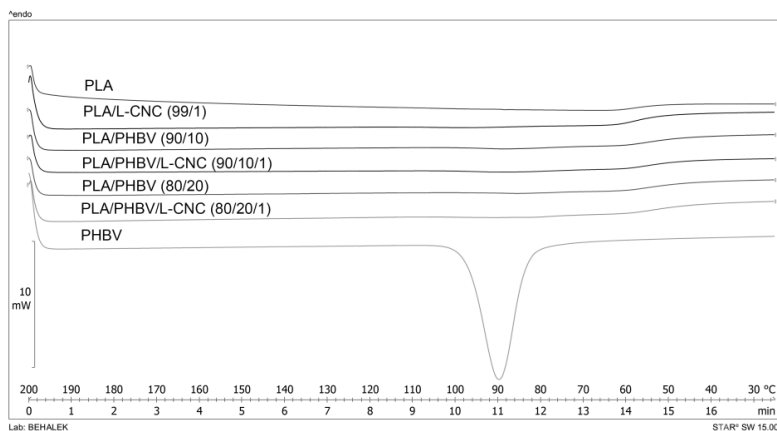


Figure 4: DSC cooling scans

Table 2: Thermal parameters of samples derived from the cooling and second heating DSC scans

	$T_m$ [°C]	$\Delta H_f$ [J·g <sup>-1</sup> ]	$\Delta H_{cc1}$ [J·g <sup>-1</sup> ]	$\Delta H_{cc2}$ [J·g <sup>-1</sup> ]	$\Delta H_C$ [J·g <sup>-1</sup> ]	$\chi_C$ (%)
PLA	169.7	29.7	24.6	0.8	0.2	4.6
PLA/L-CNC (99/1)	170.4	38.4	27.2	1.9	0.9	10.1
PLA/PHBV (90/10)	169.0	39.3	24.7	1.0	0.6	9.2 <sup>PLA</sup> 4.6 <sup>PHBV</sup>
PLA/PHBV/L- CNC (90/10/1)	169.0	38.4	23.1	1.2	1.6	12.1 <sup>PLA</sup> 4.7 <sup>PHBV</sup>
PLA/PHBV (80/20)	168.8	37.5	22.0	1.2	1.7	2.8 <sup>PLA</sup> 10.8 <sup>PHBV</sup>
PLA/PHBV/L- CNC (80/20/1)	169.1	37.2	21.2	1.1	1.0	3.2 <sup>PLA</sup> 10.9 <sup>PHBV</sup>
PHBV	171.6	84.7	-	-	69.0	77.7



## Morphology

Scanning electron microscopy (SEM) was used to study L-CNCs powder and the morphological features of pure PLA, PLA/L-CNC nanocomposites, PLA/PHBV blends and PLA/PHBV/L-CNC nanocomposite blends. The micrographs are shown in Figure 5, Figure 6 and Figure 7 respectively. Figure 5a shows L-CNCs bundle that is formed during spray drying process and its surface composed of individual L-CNCs (Figure 5b).

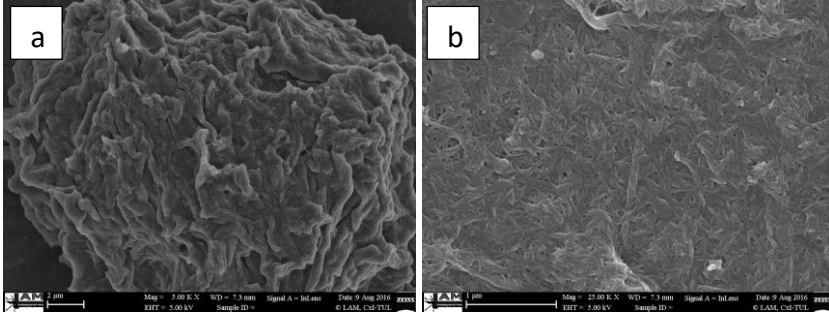


Figure 5: SEM micrographs of L-CNCs bundle (a) and individual L-CNCs on bundle surface (b)

It can be seen that pure PLA shows a typical fracture surface of an amorphous polymer (Figure 6a). In Figure 6b can be clearly seen fractured L-CNCs bundle that was insufficiently dispersed during nanocomposite processing. In this case an insufficient mechanical energy was applied to separate and disperse individual particles in viscous polymer. Limiting SEM resolution is also challenging during identification of individualized L-CNCs in fractured samples.

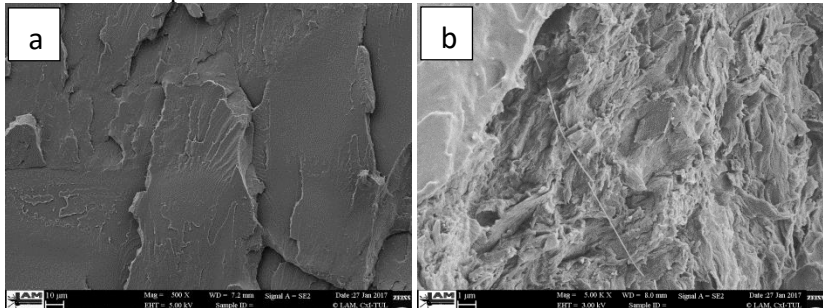


Figure 6: SEM cryo-fractured micrographs of PLA (a) and PLA/L-CNC (b) PLA/PHBV blends (Figure 7a ) and PLA/PHBV/L-CNC nanocomposite blends (Figure 7b) exhibit PHBV well dispersed in PLA phase as a small droplet like particles in nanometre range. Same phenomenon was previously observed by Gerard et al. [12]-[32]. Due to the similar structure of both polyesters, distinguishing PLA phase from PHBV phase is challenging.

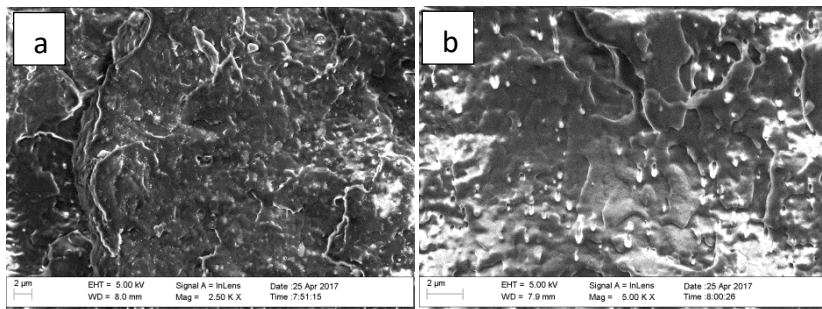


Figure 6: SEM cryo-fractured micrographs of PLA/PHBV (90/10) (a) and PLA/PHBV/L-CNC (80/20/1) (b)

### Impact properties

Pure PLA with low crystallinity degree (4.6 %) is very brittle amorphous polymer. As Figure 7 shows the impact performance of PLA can be significantly influenced by the addition of L-CNC (1 wt. %). Resulted PLA/L-CNC nanocomposites showed an increase in crystallinity (see Table 2) and impact strength over pure PLA by approx. 27 %. Nearly same result has been observed for PLA/PHBV (90/10) blends. The highest increase in impact strength by 42% over pure PLA has been observed for PLA/PHBV/L-CNC (90/10/1) nanocomposite blends. However, with higher content of minor PHBV phase (20 wt. %) impact strength of blends and nanocomposite blends started to decrease.

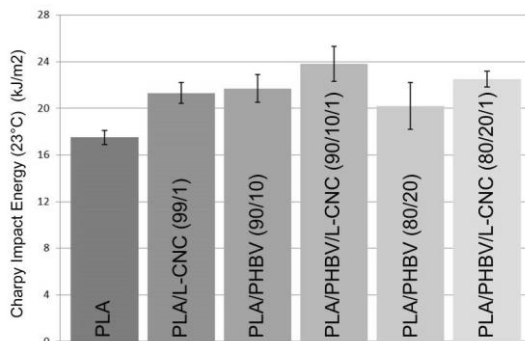


Figure 7: Unnotched (1eU) Charpy impact strength

### HDT properties

Heat Deflection Temperature (HDT) represents the upper working temperature limit of a plastic material. Method A was used (constant flexural stress of 1,80 MPa) to study resulted samples. Tsuji and Ikada [33] reported that heat resistance of pure PLA molded samples is known to be around  $T_g$ , because the crystallinity is very low under industrial molding conditions due to lower crystallization rate at higher cooling rate. This also corresponds with results of

Kawamoto, et al. [34]. As can be seen in Figure 8  $T_g$  and  $\chi_c$  are significant factors that affect HDT. With increased  $T_g$  and  $\chi_c$  (see Table 2) increased also HDT. The highest HDT has been observed for PLA/PHBV/L-CNC (90/10/1) nanocomposite blends. An increase of 16 % has been observed over pure PLA.

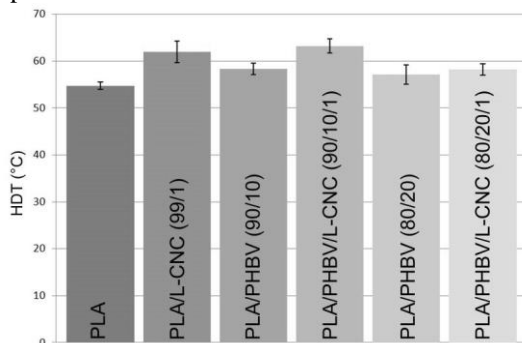


Figure 8: Heat Deflection Temperature

## Conclusion

Sustainable, biobased and biodegradable blends and nanocomposites with improved crystallinity, impact strength and heat deflection temperature have been successfully developed. The PHBV blending approach and addition of L-CNC heterogeneous nucleating agents increases the degree of crystallinity ( $\chi_c$ ) of PLA phase but also lowers the cold crystallization enthalpy ( $\Delta H_{cc}$ ) which slips to the lower temperatures or more precisely it lowers its temperature interval. At least partial miscibility occurs through shifting  $T_g$  of PLA blends and nanocomposite blends towards  $T_g$  of PHBV. Morphology studies of PLA/PHBV blends and PLA/PHBV/L-CNC nanocomposite blends exhibit PHBV well dispersed in PLA phase as a small droplet like particles in nanometre range. Inherent brittleness and low thermal stability has been improved. The highest increase in impact strength by 42% over pure PLA has been observed for PLA/PHBV/L-CNC (90/10/1) nanocomposite blends. Same material exhibited highest increase of HDT (16 %) over pure PLA.

## Acknowledgement

This paper was supported by research project SGS 21180.

## References

- [1] R. J. Moon, A. Martini, J. Nairn, J. Simonsen, and J. Youngblood, 'Cellulose nanomaterials review: structure, properties and nanocomposites', *Chem. Soc. Rev.*, vol. 40, no. 7, pp. 3941–3994 (2011).
- [2] A. P. Gupta and V. Kumar, 'New emerging trends in synthetic biodegradable polymers – Polylactide: A critique', *Eur. Polym. J.*, vol. 43, no. 10, pp. 4053–4074 (2007).
- [3] A. M. Harris and E. C. Lee, 'Improving mechanical performance of injection molded PLA by controlling crystallinity', *J. Appl. Polym. Sci.*, vol. 107, no. 4, pp. 2246–2255 (2008).
- [4] A. Jimenez, M. Peltzer, and R. Ruseckaite, *Poly (lactic acid) science and technology: processing, properties, additives and applications*. Royal Society of Chemistry (2014).
- [5] A. Pei, Q. Zhou, and L. A. Berglund, 'Functionalized cellulose nanocrystals as biobased nucleation agents in poly(L-lactide) (PLLA) – Crystallization and mechanical property effects', *Compos. Sci. Technol.*, vol. 70, no. 5, pp. 815–821 (2010).
- [6] H. Zhao, Z. Cui, X. Sun, L.-S. Turng, and X. Peng, 'Morphology and properties of injection molded solid and microcellular polylactic acid/polyhydroxybutyrate-valerate (PLA/PHBV) blends', *Ind. Eng. Chem. Res.*, vol. 52, no. 7, pp. 2569–2581 (2013).
- [7] S. Pilla, S. G. Kim, G. K. Auer, S. Gong, and C. B. Park, 'Microcellular extrusion foaming of poly(lactide)/poly(butylene adipate-co-terephthalate) blends', *Mater. Sci. Eng. C*, vol. 30, no. 2, pp. 255–262 (2010).
- [8] E. Chiellini and R. Solaro, 'Biodegradable Polymeric Materials', *Adv. Mater.*, vol. 8, no. 4, pp. 305–313 (1996).
- [9] M. R. Nanda, M. Misra, and A. K. Mohanty, 'The Effects of Process Engineering on the Performance of PLA and PHBV Blends', *Macromol. Mater. Eng.*, vol. 296, no. 8, pp. 719–728 (2011).
- [10] M. Boufarguine, A. Guinault, G. Miquelard-Garnier, and C. Sollogoub, 'PLA/PHBV Films with Improved Mechanical and Gas Barrier Properties', *Macromol. Mater. Eng.*, vol. 298, no. 10, pp. 1065–1073 (2013).
- [11] S. Khanna and A. K. Srivastava, 'Recent advances in microbial polyhydroxyalkanoates', *Process Biochem.*, vol. 40, no. 2, pp. 607–619 (2005).
- [12] T. Gerard and T. Budtova, 'Morphology and molten-state rheology of polylactide and polyhydroxyalkanoate blends', *Eur. Polym. J.*, vol. 48, no. 6, pp. 1110–1117 (2012).

- [13] I. Noda, M. M. Satkowski, A. E. Dowrey, and C. Marcott, ‘Polymer Alloys of Nodax Copolymers and Poly(lactic acid)’, *Macromol. Biosci.*, vol. 4, no. 3, pp. 269–272 (2004).
- [14] M. Zhang and N. L. Thomas, ‘Blending polylactic acid with polyhydroxybutyrate: The effect on thermal, mechanical, and biodegradation properties’, *Adv. Polym. Technol.*, vol. 30, no. 2, pp. 67–79 (2011).
- [15] E. Richards, R. Rizvi, A. Chow, and H. Naguib, ‘Biodegradable Composite Foams of PLA and PHBV Using Subcritical CO<sub>2</sub>’, *J. Polym. Environ.*, vol. 16, no. 4, pp. 258–266 (2008).
- [16] M. Niaounakis, *Biopolymers: reuse, recycling, and disposal*. Elsevier/William Andrew (2013).
- [17] S. Saaidlou, M. A. Huneault, H. Li, and C. B. Park, ‘Poly(lactic acid) crystallization’, *Prog. Polym. Sci.*, vol. 37, no. 12, pp. 1657–1677 (2012).
- [18] M. Murariu, A.-L. Dechief, R. Ramy-Ratiarison, Y. Paint, J.-M. Raquez, and P. Dubois, ‘Recent advances in production of poly(lactic acid) (PLA) nanocomposites: a versatile method to tune crystallization properties of PLA’, *Nanocomposites*, vol. 1, no. 2, pp. 71–82 (2015).
- [19] K. S. Kang, S. I. Lee, T. J. Lee, R. Narayan, and B. Y. Shin, ‘Effect of biobased and biodegradable nucleating agent on the isothermal crystallization of poly(lactic acid)’, *Korean J. Chem. Eng.*, vol. 25, no. 3, p. 599 (2008).
- [20] H. Li and M. A. Huneault, ‘Crystallization of PLA/Thermoplastic Starch Blends’, *Int. Polym. Process.*, vol. 23, no. 5, pp. 412–418, Nov (2008).
- [21] S. Kalia et al., ‘Cellulose-Based Bio- and Nanocomposites: A Review, Cellulose-Based Bio- and Nanocomposites: A Review’, *Int. J. Polym. Sci* (2011).
- [22] K. Nelson et al., ‘American Process: Production of Low Cost Nanocellulose for Renewable, Advanced Materials Applications’, in *Materials Research for Manufacturing*, L. D. Madsen and E. B. Svedberg, Eds. Springer, pp. 267–302 (2016).
- [23] A. Dufresne, ‘Nanocellulose: a new ageless bionanomaterial’, *Mater. Today*, vol. 16, no. 6, pp. 220–227 (2013).
- [24] Y. Habibi, ‘Key advances in the chemical modification of nanocelluloses’, *Chem. Soc. Rev.*, vol. 43, no. 5, pp. 1519–1542 (2014).
- [25] E. Lizundia, J. L. Vilas, and L. M. León, ‘Crystallization, structural relaxation and thermal degradation in Poly(l-lactide)/cellulose nanocrystal renewable nanocomposites’, *Carbohydr. Polym.*, vol. 123, pp. 256–265 (2015).
- [26] Y. Habibi, S. Aouadi, J.-M. Raquez, and P. Dubois, ‘Effects of interfacial stereocomplexation in cellulose nanocrystal-filled polylactide nanocomposites’, *Cellulose*, vol. 20, no. 6, pp. 2877–2885 (2013).

- [27] A. Gupta, W. Simmons, G. T. Schueneman, and E. A. Mintz, 'Lignin-coated cellulose nanocrystals as promising nucleating agent for poly(lactic acid)', *J. Therm. Anal. Calorim.*, vol. 126, no. 3, pp. 1243–1251 (2016).
- [28] M. Borůvka and P. Lenfeld, 'Extraction of cellulose nanocrystals as a potential reinforcing material for poly(lactic acid) biocomposites', presented at the NANOCON 2015 - 7th International Conference on Nanomaterials - Research and Application, Conference Proceedings, pp. 360–365 (2015).
- [29] I. Campoy, M. A. Gómez, and C. Marco, 'Structure and thermal properties of blends of nylon 6 and a liquid crystal copolyester1', *Polymer*, vol. 39, no. 25, pp. 6279–62881 (1998).
- [30] A. K. Mohanty, M. Misra, and L. T. Drzal, *Natural fibers, biopolymers, and biocomposites*. CRC Press (2005).
- [31] M. Scandola et al., 'Polymer blends of natural poly (3-hydroxybutyrate-co-3-hydroxyvalerate) and a synthetic atactic poly (3-hydroxybutyrate). Characterization and biodegradation studies', *Macromolecules*, vol. 30, no. 9, pp. 2568–2574 (1997).
- [32] T. Gérard, T. Budtova, A. Podshivalov, and S. Bronnikov, 'Polylactide/poly (hydroxybutyrate-co-hydroxyvalerate) blends: Morphology and mechanical properties', *Express Polym. Lett.*, vol. 8, no. 8, pp. 609–617 (2014).
- [33] H. Tsuji and Y. Ikada, 'Properties and morphologies of poly(l-lactide): 1. Annealing condition effects on properties and morphologies of poly(l-lactide)', *Polymer*, vol. 36, no. 14, pp. 2709–2716 (1995).
- [34] N. Kawamoto, A. Sakai, T. Horikoshi, T. Urushihara, and E. Tobita, 'Physical and mechanical properties of poly(L-lactic acid) nucleated by dibenzoylhydrazide compound', *J. Appl. Polym. Sci.*, vol. 103, no. 1, pp. 244–250 (2007).